

First Demonstration of Robust Tri-Gate β -Ga₂O₃ Nano-membrane Field-Effect Transistors Operated Up to 400 °C

Hagyoul Bae¹, Tae Joon Park², Jinhyun Noh¹, Wonil Chung¹,
Mengwei Si¹, Shriram Ramanathan², and Peide D. Ye^{1,*}

¹School of Electrical and Computer Engineering and Birck Nanotechnology Center, ²School of Materials Engineering,
Purdue University, West Lafayette, IN 47907 USA

Email: yep@purdue.edu

Abstract—Nano-membrane tri-gate β -gallium oxide (β -Ga₂O₃) field-effect transistors (FETs) on SiO₂/Si substrate fabricated via exfoliation have been demonstrated for the first time. By employing electron beam lithography, the minimum-sized features can be defined with a 50 nm fin structure. For high-quality interface between β -Ga₂O₃ and gate dielectric, atomic layer-deposited 15-nm-thick aluminum oxide (Al₂O₃) was utilized with Tri-methyl-aluminum (TMA) self-cleaning surface treatment. The fabricated devices demonstrate extremely low subthreshold slope (SS) of 61 mV/dec, high drain current (I_{DS}) ON/OFF ratio of 1.5×10^9 , and negligible transfer characteristic hysteresis. We also experimentally demonstrated robustness of these devices with current–voltage (I – V) characteristics measured at temperatures up to 400 °C.

Index Terms—Tri-gate, β -Ga₂O₃ FETs, exfoliation, wide bandgap, atomic layer deposition, single-fin, multi-fin

I. INTRODUCTION

β -Ga₂O₃ is one of the promising materials for next-generation power electronics owing to its ultra-wide bandgap of 4.6–4.9 eV, high breakdown electric field of 8 MV/cm, high electron mobility of 100–150 cm²/V·s, and sustainability for high-temperature operation and mass production with low-cost fabrication [1]–[8]. In addition, the β -Ga₂O₃ material has a higher Baliga’s figure-of-merit (FOM) than that of silicon carbide (SiC) and gallium nitride (GaN) [9], [10]. Owing to these advantages, monolithic β -Ga₂O₃ transistors could also be considered for high-temperature operation in harsh environments. In particular, stable operation of electronic devices in severe conditions, mainly at high temperatures, is indispensable for many applications in the defense, automotive, nuclear instrumentation, and aerospace fields [11], [12]. Recently, several studies have demonstrated improved electrical performances of β -Ga₂O₃ FETs by using double-gate [13], multi-channel with wrap-gate [14], vertical channel [15], back-gate [16], and recessed-gate [17], [18] devices. In particular, among these advanced technologies, structure innovation to enhance gate controllability to boost higher current density and suppress interface or short-channel effect becomes critical during device research [19]–[20]. There are still opportunities to achieve better switching characteristics, higher integration density, and lower power consumption in β -Ga₂O₃ materials and device development.

In this study, the fabrication and performance of tri-gate β -Ga₂O₃ FETs with single and multi-fin channel structures formed from nano-membranes are presented. In the single fin-structure, a narrow channel with a fin width (W_{fin}) of 50 nm is fabricated to exploit the high ON/OFF ratio of I_{DS} and superior subthreshold slope, while maintaining reliable performance at temperature from room temperature (RT) to 400 °C.

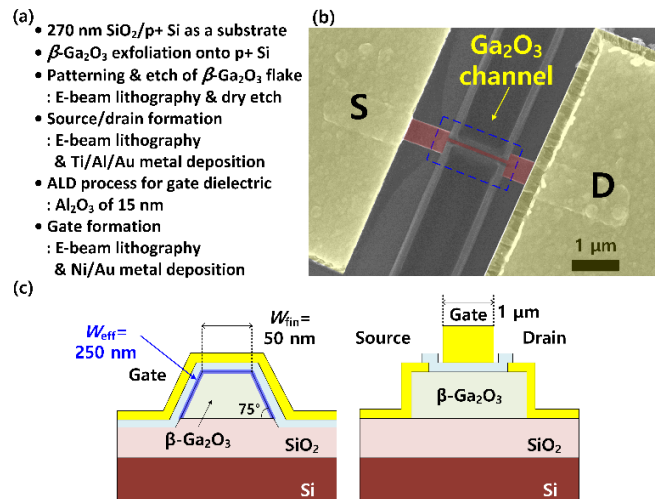


Fig. 1. (a) Process flow for device fabrication of exfoliated tri-gate β -Ga₂O₃ nano-membrane FETs with the top-gate structure. (b) SEM image of a fabricated device. (c) Cross-sectional schematics along both channel width and length directions.

II. DEVICE FABRICATION

Fig. 1(a) lists the key fabrication steps for the tri-gate nano-membrane β -Ga₂O₃ FETs on the SiO₂/Si substrate. For the fabrication of the top-gate devices, thin (100) β -Ga₂O₃ nano-membranes with a Sn doping concentration of 2.7×10^{18} cm⁻³ was transferred from the bulk β -Ga₂O₃ substrate onto a p+ Si wafer with a 270 nm SiO₂ as gate dielectric. The fin-shape active channel region was defined by electron (e)-beam lithography and the dry-etch process. To form narrower β -Ga₂O₃ fin structure, we used a BCl₃/Ar gas mixture in an inductively coupled plasma-reactive ion etching (ICP-RIE) system (Panasonic E620 Etcher) for 15 min [21]. The etching

rate of (100) β -Ga₂O₃ is about 10 nm/min under process conditions: RF power of 100 W; BCl₃ flow of 15 sccm; Ar flow of 60 sccm; and pressure of 0.6 Pa. Subsequently, the source (S) and drain (D) regions were formed via e-beam lithography patterning, Ti/Al/Au (15 /60 /50 nm) metallization, and lift-off process. No post-deposition thermal annealing was performed. By employing the atomic layer deposition (ALD) process, high-quality Al₂O₃ gate dielectric was deposited to minimize gate leakage current and high-quality interface by self-cleaning effect using TMA as the precursor [22], [23]. Subsequently, e-beam lithography was carried out for gate patterning and Ni/Au (50 /80 nm) metal gate was deposited via an e-beam evaporator. Fig. 1(b) presents the scanning electron microscope (SEM) image showing the etched β -Ga₂O₃ channel with W_{fin} of 50 nm, a gate length (L_G) of 1 μm , and a fin height (H_{fin}) of 95 nm. As the fabricated device has a 3D fin structure, the total effective channel width (W_{eff}) is approximately 250 nm, which is 5 times wider than the footprint W_{fin} of 50 nm. Fig. 1(c) shows the cross-sectional view of the fabricated device along both channel width and length directions. Using atomic force microscopy (AFM), the measured physical thickness of the exfoliated β -Ga₂O₃ nano-membrane is approximately 95 nm.

III. EXPERIMENTAL RESULTS AND DISCUSSION

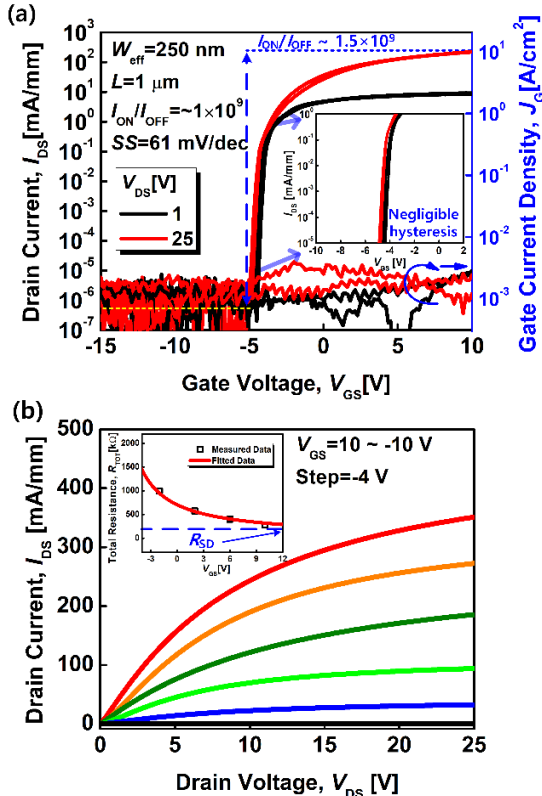


Fig. 2. (a) Measured $I_{\text{DS}}-V_{\text{GS}}$ transfer characteristics and (b) $I_{\text{DS}}-V_{\text{DS}}$ output characteristics of the fabricated tri-gate β -Ga₂O₃ FET.

Fig. 2 (a) shows the measured transfer characteristics ($I_{\text{DS}}-V_{\text{GS}}$) of the fabricated tri-gate β -Ga₂O₃ FET with W_{eff} of 250 nm and L_G of 1 μm , showing the following excellent electrical performances: 1) $I_{\text{ON}}=350$ mA/mm normalized with the W_{eff} ; 2) $I_{\text{ON}}/I_{\text{OFF}}=1.5\times 10^9$; 3) $SS_{\text{min}}=61$ mV/dec; 4) DIBL=12 mV/V; 5) $V_{\text{hys}}=30$ mV. The electrical characterizations were performed using a Keysight B1500 semiconductor parameter analyzer, a Keithley 4200-SCS parameter analyzer with a high-temperature measurement system (Micromanipulator H1000 Thermal Chuck System), and a Cascade Summit probe station. Fig. 2 (b) shows the measured output characteristics ($I_{\text{DS}}-V_{\text{DS}}$) as a function of V_{GS} from 0 to -20 V. A maximum drain current density ($I_{\text{DS,max}}$) of 350 mA/mm in the fabricated device on the SiO₂/Si substrate is obtained, which is higher than that obtained in our previous study of top-gate devices on SiO₂/Si substrate [24]. This proposed fin structure enables to control β -Ga₂O₃ channel from three sides of the gate and improve the gate electrostatics significantly as in Si CMOS technology. The threshold voltage (V_{T}) is determined to be -2.8 V by the constant current method. The parasitic source/drain resistances (R_{SD}) is obtained by extrapolating V_{GS} based on channel resistance method (CRM) as shown in the inset of Fig. 2 (b) [25]. The R_{C} and sheet resistance (R_{SH}) is extracted to be 8.0 $\Omega\cdot\text{mm}$ and 6.2 $\text{k}\Omega/\square$, respectively. Further studies on β -Ga₂O₃ contacts are highly demanded in the development of β -Ga₂O₃ device technology [26].

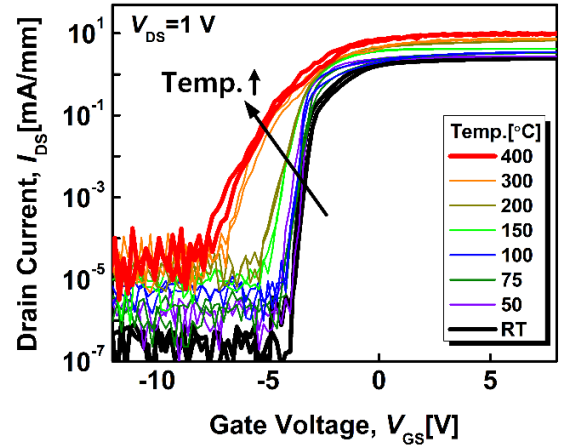


Fig. 3. Measured $I_{\text{DS}}-V_{\text{GS}}$ characteristics of the fabricated tri-gate β -Ga₂O₃ FETs on SiO₂/Si substrate at various temperatures ranging from RT to 400 $^{\circ}\text{C}$.

The measured $I_{\text{DS}}-V_{\text{GS}}$ characteristics of the fabricated tri-gate β -Ga₂O₃ FET on the SiO₂/Si substrate measured at various temperatures ranging from RT to 400 $^{\circ}\text{C}$ are shown in Fig. 3 with negligible hysteresis. Although I_{OFF} starts to gradually increase as the temperature increases, our proposed tri-gate β -Ga₂O₃ FETs have more stable characteristics for temperatures up to 400 $^{\circ}\text{C}$ compared to previous results [6], [13]. The variations in the extracted SS , V_{T} , field-effect mobility (μ_{FE}), and $I_{\text{ON}}/I_{\text{OFF}}$, as a function of temperature are plotted in Fig. 4. The value of SS increases from 61 mV/dec to 710 mV/dec and V_{T} shifts toward a negative direction due to thermally excited

carriers from interface states between the channel and the gate dielectric, as shown in Fig. 4 (a) and (b). The interface trap density (D_{it} [$\text{eV}^{-1}\text{cm}^{-2}$]) of the fabricated devices is extracted to $1.0 \times 10^{11} \text{ eV}^{-1}\text{cm}^{-2}$ at RT. The significant increase of SS beyond Boltzmann thermal limit indicates a large amount D_{it} of $1.6 \times 10^{13} \text{ eV}^{-1}\text{cm}^{-2}$ could be activated at 400°C . In addition, μ_{FE} decreases also due to the increased D_{it} at the interface and the phonon scattering in channel at high temperatures as shown in Fig. 4 (c) [6], [13], [27]. We should also note that, even at 400°C , I_{ON}/I_{OFF} was observed to be approximately 3×10^5 , as shown in Fig. 4 (d). The tri-gate $\beta\text{-Ga}_2\text{O}_3$ FETs with ALD Al_2O_3 as gate dielectric demonstrate robust electrical performances at high temperatures. Furthermore, the measured I - V characteristics at RT were again obtained after cooling the device from high temperature to RT.

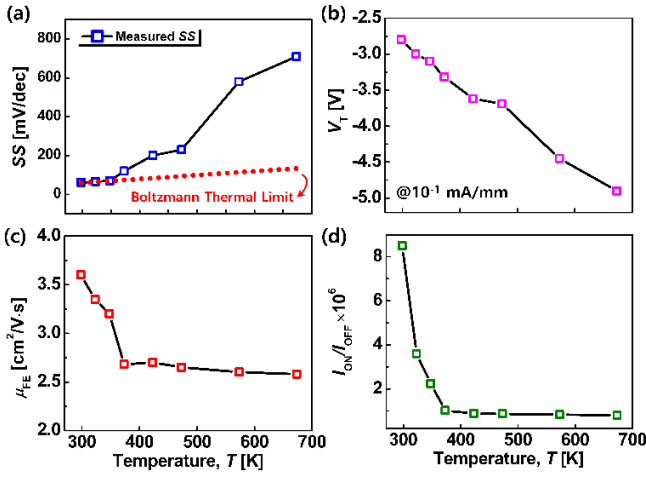


Fig. 4. Temperature dependences (RT– 400°C) at $V_{DS} = 1 \text{ V}$ of typical device parameters such as (a) SS (dashed line: Boltzmann thermal limit of SS), (b) V_T , (c) μ_{FE} , and (d) I_{ON}/I_{OFF} of the tri-gate $\beta\text{-Ga}_2\text{O}_3$ FETs on the SiO_2/Si substrate.

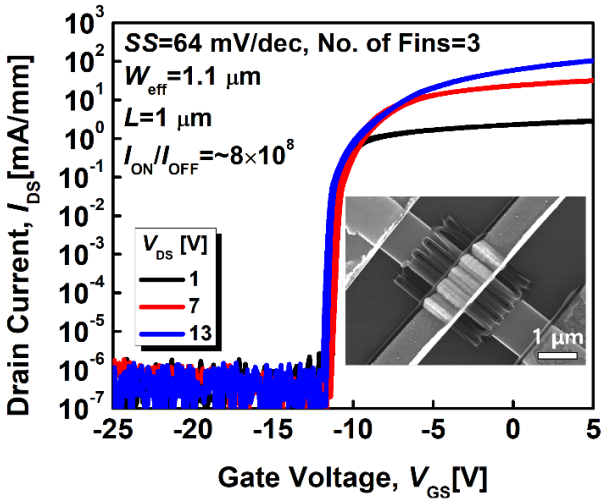


Fig. 5. Measured I_{DS} - V_{GS} characteristics of the fabricated $\beta\text{-Ga}_2\text{O}_3$ FETs with multi-fins. Inset shows SEM image for top view of the fabricated device with 3 fins.

IV. EXPERIMENTAL RESULTS AND DISCUSSION

As shown in Fig. 5, we also demonstrated the feasibility of the multi-fin tri-gate $\beta\text{-Ga}_2\text{O}_3$ FETs for a high integration density. The inset shows the SEM image for top view of the fabricated device with 3 fin channels. In case of multi-fin devices, overall device performances are also comparable to the single-fin devices. To provide clear evidences for advantages of tri-gate $\beta\text{-Ga}_2\text{O}_3$ FETs, we fabricated three types of devices with different gate structures ((i) tri-gate, (ii) planar-gate, and (iii) bottom-gate) under same process conditions and investigated the impact of the tri-gate $\beta\text{-Ga}_2\text{O}_3$ FETs via comparison with other devices, as shown in Fig. 6. Table 1 shows the comparison data of the fabricated devices with different gate structures. It is noteworthy that the tri-gate $\beta\text{-Ga}_2\text{O}_3$ FETs have high channel ratio (W_{eff} /perimeter of channel width (W_{peri})) of 0.85 and aspect ratio (AR) of 2 resulting in better electrical performances such as I_{ON}/I_{OFF} , SS , and D_{it} [28], [29]. In this regard, minimizing the device degradation caused by interface states and modulating the effective charges from $\beta\text{-Ga}_2\text{O}_3$ channel in tri-gate $\beta\text{-Ga}_2\text{O}_3$ FETs can be important since the switching characteristics are very strongly influenced by interface between $\beta\text{-Ga}_2\text{O}_3$ and bottom SiO_2 substrate.

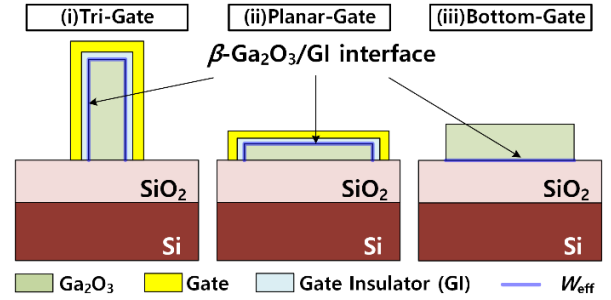


Fig. 6. Schematics of cross-sectional view for the fabricated devices with different gate structures: (i) tri-gate, (ii) planar-gate, (iii) bottom-gate.

TABLE 1
Comparison Data with Different Gate Structures

@ $V_{DS}=1 \text{ V}$	Sample #1	Sample #2	Sample #3
Structure	Single Fin	Planar	Bottom-Gate
Gate Dielectric	Al_2O_3	Al_2O_3	SiO_2
I_{ON}/I_{OFF}	$\sim 1.3 \times 10^7$	$\sim 9.5 \times 10^6$	$\sim 1.2 \times 10^6$
SS_{min} [mV/dec]	61	100	250
Type	Flake	Flake	Flake
D_{it} [$\text{eV}^{-1}\text{cm}^{-2}$]	$\sim 1 \times 10^{11}$	$\sim 9 \times 10^{11}$	$\sim 1 \times 10^{12}$
W_{eff}	250 nm	1 μm	1.5 μm
Channel Ratio (W_{eff}/W_{peri})	0.85	0.55	0.45
Aspect Ratio (AR)	2	0.12	0.1

A benchmark of the fabricated tri-gate $\beta\text{-Ga}_2\text{O}_3$ FETs is summarized in Table II. The overall electrical performances of the fabricated tri-gate $\beta\text{-Ga}_2\text{O}_3$ FETs with a single channel are improved over different types of devices reported previously.

In particular, our proposed device is highly scalable with an active channel area of $0.05 \mu\text{m}^2$ by employing an extremely scaled $\beta\text{-Ga}_2\text{O}_3$ fin structure. The D_{it} of the fabricated device shows a high-quality interface compared with previously reported results [30], [31].

TABLE 2
Benchmarking for Electrical Performances of Ga_2O_3 FETs

	This Work	Ref. [13]	Ref. [14]	Ref. [15]
I_{ON}/I_{OFF} (Max.)	$\sim 1.5 \times 10^9$	$\sim 7 \times 10^7$	$\sim 5 \times 10^5$	$\sim 1 \times 10^9$
SS_{min} [mV/dec]	61	70	158	200
# of Fin	Single	-	48	20
Type	Flake	Flake	MOVPE	Epitaxial Growth
D_{it} (Max.) [$\text{eV}^{-1}\text{cm}^{-2}$]	$\sim 1 \times 10^{11}$	-	$\sim 1 \times 10^{12}$	-
Temp.	RT~400 °C	RT~250 °C	RT	RT
V_{hys}	30 mV	30 mV	700 mV	100 mV
$I_{DS,max}$	350 mA/mm	1 mA/mm	3 mA/mm	1 kA/cm ²
W_{eff}	250 nm	7 μm	24 μm	50 μm

V. CONCLUSION

In this study, top-gate tri-gate nano-membrane $\beta\text{-Ga}_2\text{O}_3$ FETs were successfully demonstrated for the first time. Outstanding electrical performances were achieved from the single fin-like structure with a W_{fin} of 50 nm. The fabricated devices have a superior subthreshold slope and I_{ON}/I_{OFF} resulting from enhanced top gate controllability. Moreover, the fabricated devices demonstrate sustainable reliability under high temperatures of up to 400 °C, validating its use in applications involving harsh environments. Multi-fin devices also represent improved electrical performances comparable to single-fin devices for high integration density. Consequently, we expect that tri-gate $\beta\text{-Ga}_2\text{O}_3$ FETs have the potential as a low-cost and high-performance power device technology after the establishment of epitaxy materials.

REFERENCES

- [1] M. Higashiwaki and G. H. Jessen, "Guest editorial: the dawn of gallium oxide microelectronics," *Appl. Phys. Lett.*, vol. 112, no. 6, p. 060401, Feb. 2018, doi: 10.1063/1.5017845.
- [2] W. Li, K. Nomoto, Z. Hu, T. Nakamura, D. Jena, and H. G. Xing, "Single and multi-fin normally-off Ga_2O_3 vertical transistors with a breakdown voltage over 2.6 kV," in *IEDM Tech. Dig.*, Dec. 2019, pp. 270-273.
- [3] W. Xu, Y. Wang, T. You, X. Ou, G. Han, H. Hu, S. Zhang, F. Mu, T. Suga, Y. Zhang, Y. Hao, and X. Wang, "First demonstration of waferscale heterogeneous integration of Ga_2O_3 MOSFETs on SiC and Si substrates by ion-cutting process," in *IEDM Tech. Dig.*, Dec. 2019, pp. 274-277.
- [4] J. Y. Tsao, S. Chowdhury, M. A. Hollis, D. Jena, N. M. Johnson, K. A. Jones, R. J. Kaplar, S. Rajan, C. G. Van de Walle, E. Bellotti, C. L. Chua, R. Collazo, M. E. Coltrin, J. A. Cooper, K. R. Evans, S. Graham, T. A. Grotjohn, E. R. Heller, M. Higashiwaki, M. S. Islam, P. W. Juodawlkis, M. A. Khan, A. D. Koehler, J. H. Leach, U. K. Mishra, R. J. Nemanich, R. C. N. Pilawa-Podgurski, J. B. Shealy, Z. Sitar, M. J. Tadjer, A. F. Witulski, M. Wraback, and J. A. Simmons, "Ultrawide-bandgap semiconductors: research opportunities and challenges," *Adv. Elec. Mater.*, vol. 4, no. 1, p. 1600501, Jan. 2018, doi: 10.1002/aelm.201600501.
- [5] M. Higashiwaki, K. Sasaki, M. H. Wong, T. Kamimura, D. Krishnamurthy, A. Kuramata, T. Masui, and S. Yamakoshi, "Depletion-Mode Ga_2O_3 MOSFETs on $\beta\text{-Ga}_2\text{O}_3$ (010) Substrates with Si-ion-implanted channel and contacts," in *IEDM Tech. Dig.*, Dec. 2013, pp. 707-710, doi: 10.1109/IEDM.2013.6724713.
- [6] M. Higashiwaki, K. Sasaki, H. Murakami, Y. Kumagai, A. Koukitu, A. Kuramata, T. Masui, and S. Yamakoshi, "Recent progress in Ga_2O_3 power devices," *Semicond. Sci. Technol.*, vol. 31, no. 3, p. 034001, Jan. 2016, doi: 10.1088/0268-1242/31/3/034001.
- [7] S. J. Pearton, J. Yang, P. H. Cary, F. Ren, J. Kim, M. J. Tadjer, and M. A. Mastro, "A review of Ga_2O_3 materials, processing, and devices," *Appl. Phys. Rev.*, vol. 5, no. 1, p. 011301, Jan. 2017, doi: 10.1063/1.5006941.
- [8] M. Si, L. Yang, H. Zhou, and P. D. Ye, " $\beta\text{-Ga}_2\text{O}_3$ nanomembrane negative capacitance field-effect transistors with steep subthreshold slope for wide band gap logic applications," *ACS Omega*, vol. 2, no. 10, pp. 7136-7140, Oct. 2017, doi: 10.1021/acsomega.7b01289.
- [9] M. Kim, J.-H. Seo, U. Singiseti, and Z. Ma, "Recent advances in free-standing single crystalline wide band-gap semiconductors and their applications: GaN, SiC, ZnO, $\beta\text{-Ga}_2\text{O}_3$, and diamond," *J. Mater. Chem. C*, vol. 5, no. 33, pp. 8338-8354, Jun. 2017, doi: 10.1039/C7TC02211B.
- [10] M. Kim, J.-H. Seo, D. Zhao, S.-C. Liu, K. Kim, K. Lim, W. Zhou, E. Waks, and Z. Ma, "Transferrable single crystalline 4H-SiC nanomembranes," *J. Mater. Chem. C*, vol. 5, no. 2, pp. 264-268, Nov. 2016, doi: 10.1039/C6TC04480H.
- [11] J. B. Casady and R. W. Johnson, "Status of silicon carbide (SiC) as a wide-bandgap semiconductor for high-temperature applications: a review," *Solid-State Electron.*, vol. 39, no. 10, pp. 1409-1422, Oct. 1996, doi: 10.1016/0038-1101(96)00045-7.
- [12] P. G. Neudeck, R. S. Okojie, and L.-Y. Chen, "High-temperature electronics-a role for wide bandgap semiconductor?," in *Proc. IEEE*, vol. 90, no. 6, pp. 1065-1076, Nov. 2002, doi: 10.1109/JPROC.2002.1021571.
- [13] J. Ma and G. Yoo, "Low subthreshold swing double-gate $\beta\text{-Ga}_2\text{O}_3$ field-effect transistors with polycrystalline hafnium oxide dielectrics," *IEEE Electron Device Lett.*, vol. 40, no. 8, pp. 1317-1320, Aug. 2019, doi: 10.1109/LED.2019.2924680.
- [14] K. D. Chabak, N. Moser, A. J. Green, D. E. Walker, Jr., S. E. Tetlak, E. Heller, A. Crespo, R. Fitch, J. P. McCandless, K. Leedy, M. Baldini, G. Wagner, Z. Galazka, X. Li, and G. Jessen, "Enhancement-mode Ga_2O_3 wrap-gate fin field-effect transistors on native (100) $\beta\text{-Ga}_2\text{O}_3$ substrate with high breakdown voltage," *Appl. Phys. Lett.*, vol. 109, no. 21, p. 213501, Nov. 2016, doi: 10.1063/1.4967931.
- [15] Z. Hu, K. Nomoto, W. Li, N. Tanen, K. Sasaki, A. Kuramata, T. Nakamura, D. Jena, and H. G. Xing, "Enhancement-mode Ga_2O_3 vertical transistors with breakdown voltage > 1kV," *IEEE Electron Device Lett.*, vol. 39, no. 6, pp. 869-872, Apr. 2018, doi: 10.1109/LED.2018.2830184.
- [16] H. Zhou, M. Si, S. Alghamdi, G. Qiu, L. Yang, and P. D. Ye, "High-performance depletion/enhancement-mode $\beta\text{-Ga}_2\text{O}_3$ on insulator (GOOI) field-effect transistors with record drain currents of 600/450 mA/mm," *IEEE Electron Device Lett.*, vol. 38, no. 1, pp. 103-106, Jan. 2017, doi: 10.1109/LED.2016.2635579.
- [17] K. D. Chabak, J. P. McCandless, N. A. Moser, A. J. Green, K. Mahalingam, A. Crespo, N. Hendricks, B. M. Howe, S. E. Tetlak, K. Leedy, R. C. Fitch, D. Wakimoto, K. Sasaki, A. Kuramata, and G. H. Jessen, "Recessed-gate enhancement-mode $\beta\text{-Ga}_2\text{O}_3$ MOSFETs," *IEEE Electron Device Lett.*, vol. 39, no. 1, pp. 67-70, Jan. 2018, doi: 10.1109/LED.2017.2779867.
- [18] H. Dong, S. Long, H. Sun, X. Zhao, Q. He, Y. Qin, G. Jian, X. Zhou, Y. Yu, W. Guo, W. Xiong, W. Hao, Y. Zhang, H. Xue, X. Xiang, Z. Yu, H. Lv, Q. Liu, and M. Liu, "Fast switching $\beta\text{-Ga}_2\text{O}_3$ power MOSFET with a trench-gate structure," in *IEEE Electron Device Lett.*, vol. 40, no. 9, pp. 1385-1388, Sep. 2019, doi: 10.1109/LED.2019.2926202.
- [19] Y.-K. Choi, N. Lindert, P. Xuan, S. Tang, D. Ha, E. Anderson, T.-J. King, J. Bokor, and C. Hu, "Sub-20nm CMOS finfet technologies," in *IEDM Tech. Dig.*, Dec. 2001, pp. 421-424, doi: 10.1109/IEDM.2001.979526.
- [20] S. M. Kim, E. J. Yoon, H. J. Jo, M. Li, C. W. Oh, S. Y. Lee, K. H. Yeo, M. S. Kim, S. H. Kim, D. U. Choe, J. D. Choe, S. D. Suk, D.-W. Kim, D. Park, K. Kim, and B.-I. Ryu, "A novel multi-channel field effect transistor (McfET) on bulk Si for high performance sub-80nm

- application," in *IEDM Tech. Dig.*, Dec. 2004, pp. 639-642, doi: 10.1109/IEDM.2004.1419247.
- [21] L. Zhang, A. Verma, H. Xing, and D. Jena, "Inductively-coupled-plasma reactive ion etching of single-crystal β -Ga₂O₃," *Jpn. J. Appl. Phys.*, vol. 56, no. 3, p. 030304, Feb. 2017, doi: 10.7567/JJAP.56.030304.
- [22] P. D. Ye, G. D. Wilk, B. Yang, J. Kwo, S. N. G. Chu, S. Nakahara, H.-J. L. Gossmann, J. P. Mannaerts, M. Hong, K. K. Ng, and J. Bude, "GaAs metal-oxide-semiconductor field-effect transistor with nanometer thin dielectric grown by atomic layer deposition," *Appl. Phys. Lett.*, vol. 83, no. 1, pp. 180-182, Jul. 2003, doi: 10.1063/1.1590743.
- [23] C. L. Hinkle, A. M. Sonnet, E. M. Vogel, S. McDonnell, G. J. Hughes, M. Milojevic, B. Lee, F. S. Aguirre-Tostado, K. J. Choi, H. C. Kim, and R. M. Wallace, "GaAs interfacial self-cleaning by atomic layer deposition," *Appl. Phys. Lett.*, vol. 92, no. 7, p. 071901, Feb. 2008, doi: 10.1063/1.2883956.
- [24] J. Noh, S. Alajilouni, M. J. Tadjer, J. C. Culbertson, H. Bae, M. Si, H. Zhou, R. A. Bermel, A. Shakouri, and P. D. Ye, "High performance β -Ga₂O₃ nano-membrane field effect transistors on a high thermal conductivity diamond substrate," *IEEE J. Electron Devices Soc.*, vol. 7, pp. 914-918, Aug. 2019, doi: 10.1109/JEDS.2019.2933369.
- [25] H. Bae, S. Kim, M. Bae, J. S. Shin, D. Kong, H. Jung, J. Jang, J. Lee, D. H. Kim, and D. M. Kim, "Extraction of separated source and drain resistances in amorphous indium-gallium-zinc-oxide TFTs through C-V characterization," *IEEE Electron Device Lett.*, vol. 32, no. 6, pp. 761-763, Jun. 2011, doi: 10.1109/LED.2011.2127438.
- [26] K. Sasaki, M. Higashiwaki, A. Kuramata, T. Masui, and S. Yamakoshi, "Si-ion implantation doping in β -Ga₂O₃ and its application to fabrication of low-resistance ohmic contacts," *Appl. Phys. Exp.*, vol. 6, p. 086502, Aug. 2013, doi: 10.7567/apex.6.086502.
- [27] Y. Zhang, A. Neal, Z. Xia, C. Joishi, J. M. Johnson, Y. Zheng, S. Bajaj, M. Brenner, D. Dorsey, K. Chabak, G. Jessen, J. Hwang, S. Mou, J. P. Heremans, and S. Rajan, "Demonstration of high mobility and quantum transport in modulation-doped β -(Al_xGa_{1-x})₂O₃/Ga₂O₃ heterostructures," *Appl. Phys. Lett.*, vol. 112, no. 17, p. 173502, Apr. 2018, doi: 10.1063/1.5025704.
- [28] H.-W. Cheng and Y. Li, "Electrical characteristics dependence on the channel fin aspect ratio of multi-fin field effect transistors," *Semicond. Sci. Technol.*, vol. 24, no. 11, p. 115021, Oct. 2009, doi: 10.1088/0268-1242/24/11/115021.
- [29] S. H. Park, Y. Liu, N. Khariche, M. S. Jelodar, G. Klimeck, M. S. Lundstrom, and M. Luisier, "Performance comparisons of III-V and stained-Si planar FETs and nonplanar FinFETs at ultrashort gate length (12 nm)," *IEEE Trans. Electron Devices*, vol. 59, no. 8, pp. 2107-2114, Aug. 2012, doi: 10.1109/TED.2012.2198481.
- [30] H. Zhou, S. Alghamdi, M. Si, G. Qiu, and P. D. Ye, "Al₂O₃/ β -Ga₂O₃ (201) interface improvement through piranha pretreatment and postdeposition annealing," *IEEE Electron Device Lett.*, vol. 37, no. 11, pp. 1411-1414, Nov. 2016, doi: 10.1109/LED.2016.2609202.
- [31] K. Zeng, Y. Jia, and U. Singiseti, "Interface state density in atomic layer deposited SiO₂/ β -Ga₂O₃ (201) MOSCAPs," *IEEE Electron Device Lett.*, vol. 37, no. 7, pp. 906-909, Jul. 2016, doi: 10.1109/LED.2016.2570521.